

# Total variation regularization for bioluminescence tomography with an adaptive parameter choice approach

Jinchao Feng, Xiaowei Jia, Kebin Jia, Chenghu Qin, and Jie Tian\*, *FELLOW, IEEE*

**Abstract**—In this paper, we explore the application of total variation regularization method for bioluminescence tomography (BLT) with an adaptive regularization parameter choice approach. Since BLT is a seriously ill-posed problem, therefore,  $l_2$  regularized methods are frequently adopted to recover the bioluminescent sources. However,  $l_2$  regularized methods typically lead to smooth reconstructions. In this paper, we investigated the use of total variation (TV) regularization to improve the quality of BLT reconstruction. Furthermore, the regularization parameter in TV method was chosen adaptively to make the proposed algorithm more stable. Results on simulation data provide evidence that the reconstructed source can be localized accurately compared with  $l_2$  method. Meanwhile, the effectiveness of utility of the parameter choice were illustrated. Finally, different levels of noisy data were added to validate the performance of the proposed algorithm.

## I. INTRODUCTION

Molecular imaging is a sensitive, specific, quantitative, and noninvasive imaging, which is aimed at detecting, capturing, and monitoring molecular/cellular abnormalities *in vivo* that cause diseases and associated symptoms [1], [2], [3]. Optical molecular imaging, a developing modality of molecular imaging, has become an essential *in vivo* small animal tool in recent years. Bioluminescent tomography (BLT), one of most important technique of optical molecular imaging, provides a technique to study disease and treatment response in the same animal, thus offers the potential to accelerate basic research and drug discovery. The central problem for BLT is to reconstruct the underlying bioluminescent source distribution in tissue by recording tomographical data sets and employing appropriate tomographic image reconstruction schemes. However, the problem is a challenging problem since the inverse source problem is ill-posed and underdetermined and large heterogeneity in tissue optical properties caused by

This work is supported by the National Basic Research Program of China (973 Program) under Grant No. 2011CB707700, the Knowledge Innovation Project of the Chinese Academy of Sciences under Grant No. KGCX2-YW-907, the National Natural Science Foundation of China under Grant No. 30970780, 81000624, 81027002, 81071205, the Hundred Talents Program of the Chinese Academy of Sciences, the Science and Technology Key Project of Beijing Municipal Education Commission under Grant No. KZ200910005005, the Doctoral Fund of the Ministry of Education of China under Grant No. 20091103110005, Scientific Research Foundation of BJUT under Grant No. X0002012201101.

J. Feng and K. Jia are with the College of Electronic Information & Control Engineering, Beijing University of Technology, Beijing 100124, China, kebinj@bjut.edu.cn

X. Jia is with School of Computer Science and Technology, University of Science and Technology of China, Hefei, Anhui, 230027, China,

C. Qin and J. Tian are with Intelligent Medical Research Center, Institute of Automation, Chinese Academy of Sciences, P. O. Box 2728, Beijing 100190, China, tian@ieee.org

complex tissue morphology further challenges the tomography reconstruction algorithm [4], [5].

Wang et al. established a mathematical foundation on the uniqueness for reconstruction of a bioluminescent source distribution in BLT [4]. Based on the foundation, various reconstruction algorithms have largely focused on solving the ill-posed inverse problem. In particular, it is becoming increasingly common to incorporate *a priori* information to reduce the ill-posedness and improve the quantitative accuracy of BLT reconstruction. Initially, *a priori* permissible source region strategy is used to constrain the possible solution by combining other anatomic imaging modality such as magnetic resonance imaging (MRI) and computed tomography (CT) [6], [7], [8], [9], [10]. And variations in the permissible source region strategies are also reported [11], [12]. Recently, the importance of spectrally-resolved BLT has been realized and using measurements of a single wavelength can lead to multiple solutions of internal bioluminescent source distribution [13], [14], [15]. The spectrum of the bioluminescent source as *a priori* information can improve the reconstructed results largely.

Utilizing the above mentioned *a priori* information, the BLT problem can be finally converted to minimize an objective function with a quadratic ( $l_2$ ) data fidelity term and a regularizer. Typically, the regularizer is  $l_2$  norm, or named as *Tikhonov term*. In general  $l_2$  norm tends to penalize the large elements and create spurious small elements which over-smooths the reconstructed images. However, the total variation (TV) regularization can take care of the edge information of the recovered image, and thus usually obtains much better results than the  $l_2$  regularized methods [16].

As for regularization methods, the choice of the regularization parameter has a profound effect on the reconstruction quality of BLT because regularization parameter controls the smoothness of the regularized solution and balances the influence of the noise. The most straightforward and most popular-method to choose the parameter is to examine solutions for a range of regularization parameter heuristically by eye and to select the one that results in the most acceptable reconstruction [17]. But the method is subjective and non-repeatable [17], [18]. In addition, it is time-consuming and usually requires trial-and-error. In spite of the importance of regularization parameter, the method for selecting regularization parameter has not received much attention in BLT.

In this paper, we investigated a TV regularization method for BLT and addressed an adaptive regularization parameter choice strategy. To our knowledge, no results have been

reported for TV method with automatic regularization parameter in BLT, even in optical molecular tomography. Finally, the feasibility and the effectiveness of the proposed were evaluated by the simulation experiments.

## II. METHODS

### A. Forward model for BLT

In bioluminescence imaging, regarding the forward model of photon migration, radiative transfer equation (RTE) is regarded as a golden standard. However, considering its difficult to be solved and computational burden, in practise, the most popular forward model is its diffusion approximation (DA). Assuming the bioluminescent source density is stable when photons are collected, then the steady-state diffusion equation and Robin boundary condition can be used to model the propagation of photons in biological tissues [19], [20]. Taking the influence of light wavelength  $\lambda$  on tissue optical property into account, the following model is given [21]:

$$\begin{aligned} -\nabla \cdot (D(\mathbf{r}, \lambda) \nabla \Phi(\mathbf{r}, \lambda)) + \mu_a(\mathbf{r}, \lambda) \Phi(\mathbf{r}, \lambda) &= S(\mathbf{r}, \lambda) \\ (\mathbf{r} \in \Omega) \quad (1) \\ \Phi(\mathbf{r}, \lambda) + 2A(\mathbf{r}; n, n') D(\mathbf{r}, \lambda) (\nu(\mathbf{r}, \lambda) \cdot \nabla \Phi(\mathbf{r}, \lambda)) &= 0 \\ (\mathbf{r} \in \partial\Omega) \quad (2) \end{aligned}$$

where  $\Omega$  is a bounded smooth domain in the three-dimensional Euclidean space  $R^3$  that contains an object to be imaged;  $\partial\Omega$  is the corresponding boundary;  $\Phi(\mathbf{r}, \lambda)$  denotes the photon flux density [Watts/mm<sup>2</sup>];  $S(\mathbf{r}, \lambda)$  is the bioluminescent source density [Watts/mm<sup>3</sup>];  $\mu_a(\mathbf{r}, \lambda)$  is the absorption coefficient [mm<sup>-1</sup>];  $D(\mathbf{r}, \lambda) = 1/(3(\mu_a(\mathbf{r}, \lambda) + (1-g)\mu_s(\mathbf{r}, \lambda)))$  is the optical diffusion coefficient,  $\mu_s(\mathbf{r}, \lambda)$  the scattering coefficient [mm<sup>-1</sup>], and  $g$  the anisotropy parameter;  $\nu(\mathbf{r})$  the unit outer normal on  $\partial\Omega$ . Given the mismatch between the refractive indices  $n$  for  $\Omega$  and  $n'$  for the external medium,  $A(\mathbf{r}; n, n')$  can be approximately represented:

$$A(\mathbf{r}; n, n') \approx \frac{1 + R(\mathbf{r})}{1 - R(\mathbf{r})} \quad (3)$$

where  $n'$  is close to 1.0 when the mouse is in air;  $R(\mathbf{r})$  can be approximated by  $R(\mathbf{r}) \approx -1.4399n^{-2} + 0.7099n^{-1} + 0.6681 + 0.0636n$  [22]. The measured quantity is the outgoing flux density  $Q(\mathbf{r}, \lambda)$  on boundary  $\partial\Omega$  and it can be expressed:

$$Q(\mathbf{r}, \lambda) = -D(\mathbf{r}) (\nu \cdot \nabla \Phi(\mathbf{r}, \lambda)) = \frac{\Phi(\mathbf{r}, \lambda)}{2A(\mathbf{r}; n, n')} (\mathbf{r} \in \partial\Omega) \quad (4)$$

In BLT experiments, the outgoing flux density can be detected with a group of bandpass filters, so the continuous spectral range of bioluminescence light can be divided into  $m$  bands  $\tau_1, \dots, \tau_m$ , with  $\tau_l = [\lambda_{l-1}, \lambda_l], l = 1, 2, \dots, m$ . Here  $\lambda_0 < \lambda_1 < \dots < \lambda_m$  is a partition of the spectrum range. Calculation of multispectral forward model requires solution for the monochromatic case for each wavelength  $\tau_l$ . Since finite element method can easily deal with the complex boundary and biological tissues, finite element method is applied to compute the forward model for each band  $\tau_l$  [23]. We use the vector  $\mathbf{x}$  to denote the set of unknown source density. Finally, a vector function  $f(\mathbf{x})$  is obtained

by integrating the monochromatic models over the source spectrum [10], [11], [12].

### B. TV regularization algorithm

The BLT problem is an ill-posed inverse problem, and the unique solution of BLT has been theoretically proved. Generally, to reconstruct the bioluminescence source, the popular way is to formulate BLT as a least-square minimization problem with  $l_2$  regularization term, i.e.,

$$\min_{\mathbf{x} \geq \mathbf{0}} \mathcal{H}(\mathbf{x}) = \|\mathbf{y} - f(\mathbf{x})\|_2^2 + \gamma \|\mathbf{x}\|_2 \quad (5)$$

where  $\mathbf{y}$  is the multispectral boundary measured data,  $\mathbf{y} = [\mathbf{y}(\tau_1), \mathbf{y}(\tau_2), \dots, \mathbf{y}(\tau_m)]^T$ . And  $\gamma$  is regularization parameter. However, the  $l_2$ -based reconstruction algorithm can over-smooth the reconstructed results. And the recently research reveals that reconstructed results can benefit from TV-based reconstruction algorithms. Therefore, we regularize TV norm instead of  $l_2$  norm as follow

$$\min_{\mathbf{x} \geq \mathbf{0}} \mathcal{L}(\mathbf{x}) = \|\mathbf{y} - f(\mathbf{x})\|_2^2 + \gamma \|\mathbf{x}\|_{TV} \quad (6)$$

where  $\|\cdot\|_{TV}$  denotes the TV norm, which can be defined as

$$\|\mathbf{x}\|_{TV} := \int |\nabla \mathbf{x}| d\mathbf{r} \quad (7)$$

Based on finite element method,  $\|\mathbf{x}\|_{TV}$  can be simply converted in the following matrix form [24], that is

$$\|\mathbf{x}\|_{TV} = \|D\mathbf{x}\|_1 \quad (8)$$

### C. Adaptive regularization parameter choice strategy

For regularization method, the choice of regularization parameter is crucial. To estimate the regularization parameter  $\gamma$  in an efficient manner, an iterative algorithm was investigated in this paper, which was developed based on the balancing principle derived by the model function approach [16].

Given an initial guess  $\gamma_0$ , generate a sequence of  $\gamma_1, \gamma_2, \dots$  according to

$$\gamma_{k+1} = (\alpha - 1) \frac{\|\mathbf{y} - f(\mathbf{x}_k)\|_2^2}{\|D\mathbf{x}_k\|_1} \quad (9)$$

where  $\alpha$  is a positive number and  $\alpha$  satisfies  $\alpha > 1$ ,  $\mathbf{x}_k$  represents the reconstructed source distribution for the given  $\gamma_k$ . When  $|(\gamma_{k+1} - \gamma_k)/\gamma_{k+1}| < tol$  or  $k \geq K_{max}$ , the iteration terminates, where  $tol$  is a small positive number and  $K_{max}$  the maximum iterative number.

## III. RESULTS

To validate the proposed algorithm, numerical simulations are performed on a 2D circle with 10 mm radius. For the simulated measurements, two bands (600 nm and 630 nm) were adopted. And the corresponding optical parameters could be found from the literature [14]. In order to avoid the ‘‘inverse crime’’, the measured data was generated on a finer mesh which was different from the mesh used in reconstruction. Approximately 1300 variables need to be recovered using 250 measurements. Three bioluminescent sources with 2 mm diameter was centered at (-5 mm, 0 mm), (0 mm, 5 mm) and (5 mm, -5 mm).

### A. Comparisons between TV and $l_2$ regularization

In this section, to illustrate the performances of TV and  $l_2$  regularization, the regularization parameter used in this section was fixed as a constant, and its value was set to  $\gamma = 1.0 \times 10^{-8}$ . The  $l_2$  regularized reconstruction was shown in Fig. 1(a). For the TV reconstruction, the result was shown in Fig. 1(b). It is clearly visible that the  $l_2$  reconstruction exhibits artifacts near the bioluminescent sources which degrades image quality significantly. Meanwhile, the reconstructed sources were hardly distinguished from the other sources, which revealed a bad spatial resolution for  $l_2$  reconstruction.

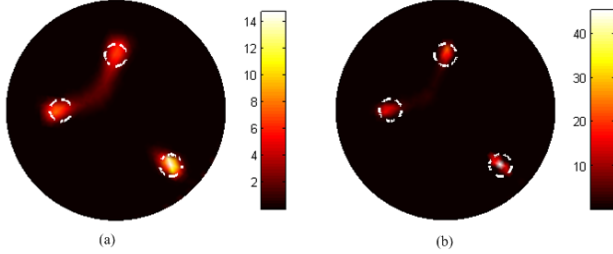


Fig. 1. The comparison between  $l_2$  and TV regularization. (a) is the result with  $l_2$  reconstruction; (b) is the result with TV reconstruction. The white circle denotes the actual source position.

### B. Validation of adaptive regularization parameter

For choosing the regularization parameter,  $\alpha$  and  $tol$  were set to 1.05 and  $6.0 \times 10^{-2}$ . As for the initial value of  $\gamma_0$ , we set to  $\gamma_0 = 0.8 * \|A^T \mathbf{y}\|$ , where  $A$  is the system matrix. The maximum iterative number  $K_{max}$  was 10. The iteration was terminated after 8 iterations, and the estimated regularization parameter was  $1.03 \times 10^{-5}$ . Figure 2 shows the evolution results at  $k$ th iteration. From the figure, we can see that the regularization parameter has an important influence on the reconstructed images. The reconstructed result was poor with the initial value  $\gamma_0 = 5.90 \times 10^{-2}$ , and the sources were not located accurately. As the number of iterations increased, the estimated parameter was approach to the real value, so the reconstructed sources were located accurately and the image quality could be improved greatly. Although there exists an artifact in the Fig. 2(e)-(h), the artifact can be removed by choosing proper threshold since its value is much small than that of other sources.

### C. Influence of data noise

The performance of the proposed algorithm was analyzed with noisy data, and the noisy measurements ( $\mathbf{y}_{noise}$ ) were obtained by:

$$\mathbf{y}_{noise} = \mathbf{y} + \frac{N}{100} * n * \mathbf{y} \quad (10)$$

where  $N$  denotes the digital number of percentage of noise, and  $n$  is the random numbers which varies between  $-1$  and  $1$ .

Fig. 3 shows the images reconstructed with  $l_2$  and TV regularization at 1%, 3%, 5% and 10% noise levels, respectively. As seen from the figure, TV regularization can

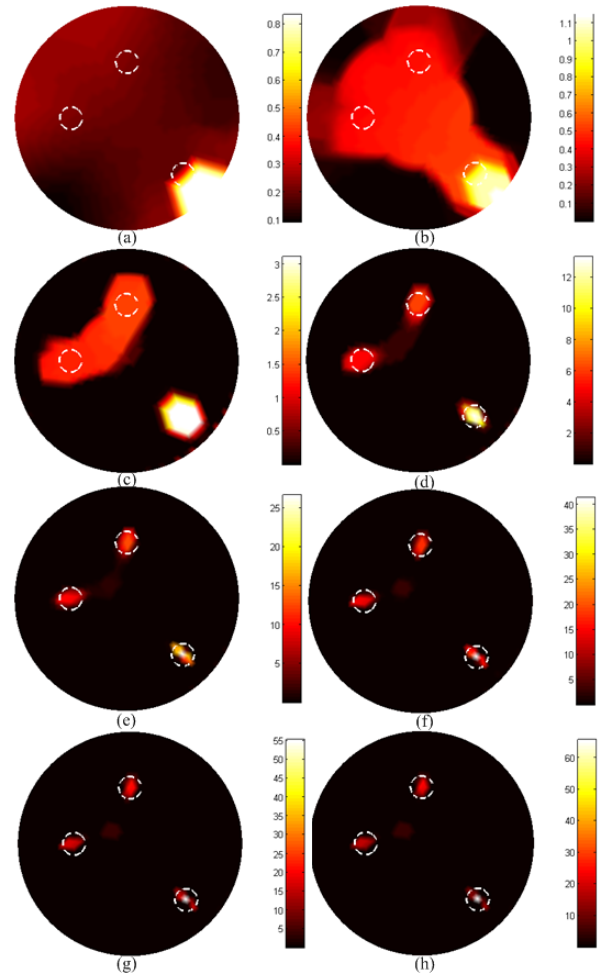


Fig. 2. The evolution reconstructed results with automatic regularization parameter choice strategy. (a)-(h) are the results at  $k$ th iteration. The white circle denotes the actual source position.

TABLE I

THE ESTIMATED REGULARIZATION PARAMETER FOR DIFFERENT NOISE LEVELS IN FIG. 3.

Noise level	The estimated $\gamma$	The iteration number
1%	$1.43 \times 10^{-5}$	9
3%	$2.81 \times 10^{-5}$	8
5%	$5.06 \times 10^{-5}$	8
10%	$1.29 \times 10^{-5}$	8

all exhibit good image quality than the images obtained using the  $l_2$  regularization and the images of  $l_2$  method are over-smoothed. As the results indicate, TV regularization is stable with noisy measurements. Note that the regularization parameters were selected automatically, which were listed in Table I and the required iterative numbers were also compiled in the table.

## IV. CONCLUSION

Bioluminescence tomography suffers from the low resolution compared with computed tomography due to its diffusion nature. Generally, to recover the bioluminescent source, regularization is indispensable. However, the reconstructed

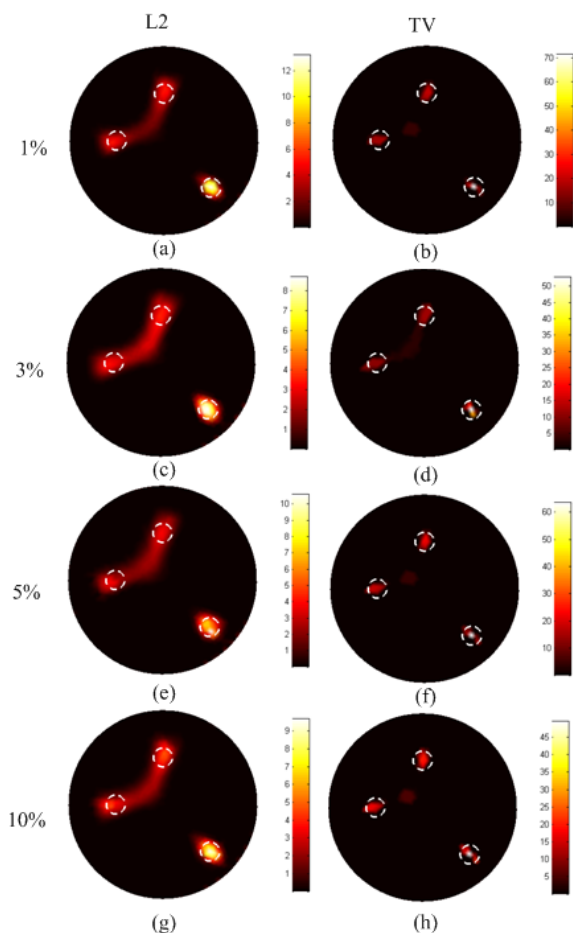


Fig. 3. The results reconstructed with noisy data. The images of the first column are with 1% noise, the second and third rows with 3% and 5% noise, and 10% for the last row. The left column are the results with  $l_2$  and the right column are TV method. The white circle denotes the actual source position.

images are over-smoothed using  $l_2$  regularization term. Using TV norm as a regularization term, the reconstructed images could be improved compared with  $l_2$  norm. Additionally, the choice of regularization parameter usually requires a trial-and-error process, which limits the application and efficiency of reconstruction algorithms. In contrast, the regularization parameter used in the proposed algorithm was estimated based on an iterative method, which could be used to locate sources accurately. The proposed algorithm are stable with noisy measurement data. In the 3D case, the computational burden for TV method increase significantly, and our computer was inaccessible. Our future work will focus on parallelization of the TV regularization.

#### REFERENCES

- [1] B. W. Rice, M. D. Cable, and M. B. Nelson, "In vivo imaging of light-emitting probes," *J. Biomed. Opt.*, vol. 6, pp. 432-440, 2001.
- [2] V. Ntziachristos, J. Ripoll, L. V. Wang, and R. Weissleder, "Looking and listening to light: the evolution of whole-body photonic imaging," *Nat. Biotechnol.*, vol. 23, pp. 313-320, 2005.
- [3] G. Wang, R. J. Jaszczak, and J. P. Basilion, "Guest Editorial Toward Molecular Imaging," *IEEE Trans. Med. Imaging*, pp. 1-3, 2005.

- [4] G. Wang, Y. Li, and M. Jiang, "Uniqueness theorems in bioluminescence tomography," *Med. Phys.*, vol. 31, pp. 2289-2299, 2004.
- [5] S. C. Davis, H. Dehghani, J. Wang, S. Jiang, B. W. Pogue, and K. D. Paulsen, "Image-guided diffuse optical fluorescence tomography implemented with Laplacian-type regularization," *Opt. Express*, vol. 15(7), pp. 4066-4082, 2007.
- [6] G. Wang, E. A. Hoffman, G. McLennan, L. V. Wang, M. Suter, and J. Meinel, "Development of the first bioluminescent CT Scanner," *Radiology*, 229(P), 566, 2003.
- [7] W. Cong, G. Wang, D. Kumar, Y. Liu, M. Jiang, L. V. Wang, E. A. Hoffman, G. McLennan, P. B. McCray, J. Zabner, and A. Cong, "Practical reconstruction method for bioluminescence tomography," *Opt. Express*, vol. 13, pp. 6756-6771, 2005.
- [8] J. Feng, K. Jia, C. Qin, G. Yan, S. Zhu, X. Zhang, J. Liu, and J. Tian, "Three-dimensional bioluminescence tomography based on Bayesian approach," *Opt. Express*, vol. 17(19), pp. 16834-16848, 2009.
- [9] M. Allard, D. Côté, L. Davidson, J. Dazai, and R. M. Henkelman, "Combined magnetic resonance and bioluminescence imaging of live mice," *J. Biomed. Opt.*, vol. 12, pp. 034018-1-11, 2007.
- [10] Y. Lv, J. Tian, W. Cong, G. Wang, J. Luo, W. Yang, and H. Li, "A multilevel adaptive finite element algorithm for bioluminescence tomography," *Opt. Express*, vol. 14, pp. 8211-8223, 2006.
- [11] Y. Lv, J. Tian, W. Cong, G. Wang, W. Yang, C. Qin, and M. Xu, "Spectrally resolved bioluminescence tomography with adaptive finite element: methodology and simulation," *Phys. Med. Biol.*, vol. 52, pp. 4497-4512, 2007.
- [12] J. Feng, K. Jia, G. Yan, S. Zhu, C. Qin, Y. Lv, and J. Tian, "An optimal permissible source region strategy for multispectral bioluminescence tomography," *Opt. Express*, vol. 16, pp. 15640-15654, 2008.
- [13] G. Alexandrakis, F. R. Rannou, and A. F. Chatzizoiannou, "Tomographic bioluminescence imaging by use of a combined optical (OPET) system: a computer simulation feasibility study," *Phys. Med. Biol.*, vol. 50, pp. 4225-4241, 2005.
- [14] H. Dehghani, S. C. Davis, S. Jiang, B. W. Pogue, K. D. Paulsen, and M. S. Patterson, "Spectrally resolved bioluminescence optical tomography," *Opt. Lett.*, vol. 31, pp. 365-367, 2006.
- [15] H. Dehghani, S. C. Davis, and B. W. Pogue, "Spectrally resolved bioluminescence tomography using the reciprocity approach," *Med. Phys.*, vol. 35, pp. 4863-4871, 2008.
- [16] C. Clason, B. Jin, and K. Kunisch, "A duality-based splitting method for  $l_1$ -TV image restoration with automatic regularization parameter choice," SFB Report, Tech. Rep. 2009-041, 2009. [Online]. Available: <http://math.unigraz.at/mobis/publications/SFB-Report-2009-041.pdf>.
- [17] T. Correia, A. Gibson, M. Schweiger, and J. Hebden, "Selection of regularization parameter for optical topography," *J. Biomed. Opt.*, vol. 14(3), pp. 034044-1-11, 2009.
- [18] B. M. Graham, and A. Adler, "Objective selection of hyperparameter for EIT," *Physiol. Meas.*, vol. 27, pp. S65-S79, 2006.
- [19] S. R. Arridge, M. Schweiger, M. Hiraoka, and D. T. Delpy, "A finite element approach for modeling photon transport in tissue," *Med. Phys.*, vol. 20, pp. 299-309, 1993.
- [20] S. R. Arridge, "Optical tomography in medical imaging," *Inverse Probl.*, vol. 15, pp. 41-93, 1999.
- [21] A. J. Chaudhari, F. Darvas, J. R. Bading, R. A. Moats, P. S. Conti, D. J. Smith, S. R. Cherry, and R. M. Leahy, "Hyperspectral and multispectral bioluminescence optical tomography for small animal imaging," *Phys. Med. Biol.*, vol. 50, pp. 5421-5441, 2005.
- [22] M. Schweiger, S. R. Arridge, M. Hiraoka, and D. T. Delpy, "The finite element method for the propagation of light in scattering media: Boundary and source conditions," *Med. Phys.*, vol. 22, pp. 1779-1792, 1995.
- [23] C. Qin, J. Tian, Y. Lv, and W. Yang, "Three-dimensional Bioluminescent Source Reconstruction Method based on Nodes of Adaptive FEM," In *Medical Imaging 2008: Physiology, Function, and Structure from Medical Images*, vol. 6916, Proceedings of SPIE, 2008.
- [24] H. Gao, and H. Zhao, "Multilevel bioluminescence tomography based on radiative transfer equation Part 2: total variation and  $l_1$  data fidelity," *Opt. Express*, vol. 18, pp. 2894-2912, 2010.